Peptide Bond Ultraviolet Absorption Enables Vibrational Cold-Ion Spectroscopy of Non-aromatic Peptides.

Aleksandr Y. Pereverzev, Vladimir N. Kopysov, and Oleg V. Boyarkin[*]

Laboratoire de Chimie Physique Moléculaire, École Polytechnique Fédérale de Lausanne, Station-6, 1015 Lausanne, Switzerland

[*] Corresponding Author: oleg.boiarkin@epfl.ch

ABSTRACT

Peptide bond VUV absorption is inherent to all proteins and peptides. Although widely exploited in top-down proteomics for photodissociation, this absorption has never been spectroscopically characterized in the gas phase. We have measured VUV/UV photofragmentation spectrum of a single peptide bond in a cryogenically cold protonated dipeptide. Although the spectrum appears to be very broadband and structureless, vibrational pre-excitation of this and even larger cold peptides significantly increases the UV dissociation yield for some of their photofragments. We use this effect to extend the technique of IR-UV photofragmentation vibrational spectroscopy, developed for aromatic peptides, to non-aromatic ones and demonstrate measurements of conformation specific and non-specific IR spectra for di- to hexa-peptides.

TOC GRAPHICS

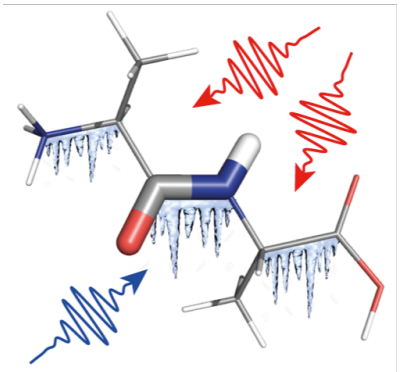

Vibrational spectroscopy of cold biological ions is a proven method for unambiguous conformational assignment of their calculated intrinsic structures. IR-UV double-resonance photofragmentation technique allows for recording conformer-specific vibrational spectra of protonated aromatic species as large as decapeptides[1-2] and their microsolvated complexes[3], provided their electronic spectra are vibrationally resolved. In the cases when a short lifetime of the excited electronic state and/or a substantial spectral congestion preclude vibrational resolution in UV spectra of ions, IR-IR-UV hole-burning technique may allow for conformational assignment of the resolved vibrational transitions in IR spectra.[4-8] Regardless of the case, both techniques are applicable to only those peptides that contain at least one aromatic residue, which serves for UV-induced photofragmentation. Although large polypeptides and proteins are very likely to contain aromatics, many small to midsize oligopeptides, for which IR spectroscopy is most informative, have no chromophores. Regarding the natural abundance of Phe (4%), Tyr (3.3%), His (2.9%), and Trp (1.3%) aromatic amino acids, the chance that, for instance, a pentapeptide has none of them is about 56%. This implies that vibrational spectra of a good fraction of oligopeptides isolated in the gas phase could not be probed by IR-UV approach.

IRMPD spectroscopy allows for measurements of vibrational spectra of non-aromatic peptides.[9] Although simple, this technique lacks conformational specificity, which is highly desired for structural analysis of vibrational spectra. IR-IR tagging allows for conformation specific vibrational spectroscopy of non-aromatic peptides.[10] This technique employs vibrational rather than electronic transitions to label conformers of an ion complexed with a weakly bound tag molecule. Even small low-polarizable tags, like H_2 or He, may cause noticeable changes in geometry and shifts of vibrational frequencies of ions[11] and require higher mass resolution to

detect a loss of single tags. Non-conformer selective IR tagging spectroscopy has been demonstrated for protonated molecules as large as a decapeptide[12] and the C_{60} fullerene,[13] although, to our knowledge, $[Gly_3+H]^+$ remains the largest peptide to which conformer-selective IR-IR tagging technique has been applied so far.[14] Herein we extend the conformer non-selective IR-UV and conformer-selective IR-IR-UV techniques to vibrational spectroscopy of small to midsize protonated non-aromatic oligopeptides. In addition to all the benefits of tagging approach, UV fragmentation enables mass spectrometry of the produced fragments, which may provide some supplementary structural constrains for solving geometry and/or sequence of a peptide. We, first, measure and characterize the UV/VUV absorption by a single peptide bond - a chromophore that is intrinsic to any peptide and protein. This absorption is employed for photofragmentation of cold protonated peptides, while the increase of the fragmentation yield upon IR laser pre-excitation of these ions allows for measuring their vibrational spectra.

Amide groups of peptides and proteins exhibit three major absorption bands, centred near 190 nm, 160 nm, and 130 nm, which were assigned to $\pi^* \leftarrow n$, $\pi^* \leftarrow \pi$ and $\sigma^* \leftarrow \pi$ transitions.[15-18] The first UV-induced photodissociation (UVPD) experiments that employed excitation of amide bonds at 193 nm, were reported in 1984 for several short protonated oligopeptides in the gas phase.[19 20] The main advantage of UVPD over a collisional dissociation (CID and HCD) is in producing more types of ionic fragments.[21] Despite the wide use of UVPD in top-down proteomics,[21-25] the fragmentation spectra measured by VUV/UV excitation of peptide bonds in protonated gas-phase peptides have never been reported. Figure 1a compares the measured UV/VUV photofragmentation spectra of cold (vibrational temperature of ~10 K)[26] protonated amino acid alanine ($[Ala+H]^+$, m/z = 90.1 Th) and dipeptide $[Ala_2+H]^+$ (m/z = 161.1 Th). Consistently with the known weak UV absorption of Ala in solution,[27] the fragmentation yield of

$[Ala+H]^+$ in the gas-phase is nearly hundred times lower than the yield measured for the dipeptide which contains a peptide bond. The spectrum of cold $[Ala_2+H]^+$, therefore, reflects the $\pi^* \leftarrow \pi$ transition of the O-C-N peptide bond.[15] Despite the suppression of inhomogeneous thermal broadening, the observed UV/VUV fragmentation band of the peptide bond in the isolated cold ions remains broad and vibrationally unresolved.

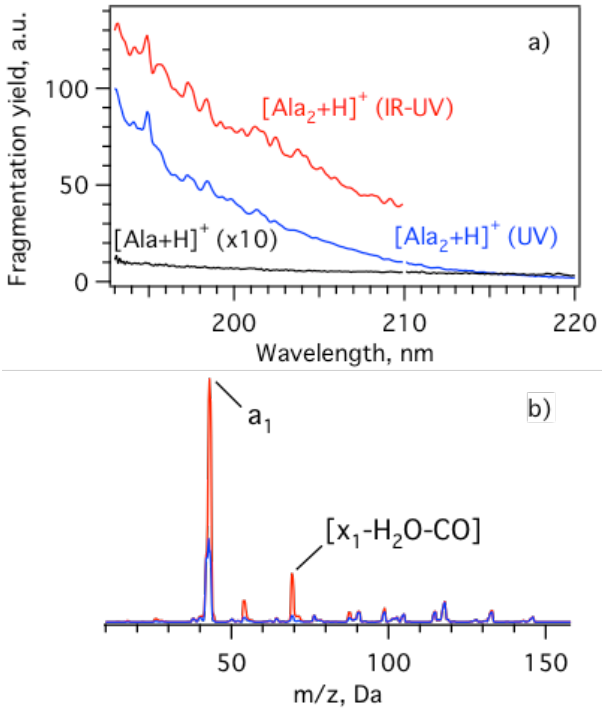

Figure 1. (**a**) Electronic spectra of cold $[Ala+H]^+$ (black trace) and $[Ala_2+H]^+$ (blue traces), and of $[Ala_2+H]^+$ vibrationally pre-excited by IR OPO tuned to 3567.2 cm^{-1} (red trace). The spectrum of $[Ala+H]^+$ was recorded by integrating the intensities of all fragments (See SI Section S1); the spectra of $[Ala_2+H]^+$ were recorded by monitoring intensity of the a_1 fragment. The spectra are normalized by parent ion signal and by laser power. (**b**) UV photofragmentation mass spectrum of cold and IR pre-excited $[Ala_2+H]^+$ (blue and red traces, respectively) measured with UV OPO wavelength fixed at 210 nm.

Conformer non-selective IR-UV gain spectroscopy records IR transitions in all abundant conformers of an ion. The technique is based on a significant increase of UV photofragmentation upon an IR pre-excitation of cold ions.[28] Figure 1a compares the measured UVPD spectra of cold and IR pre-excited $[Ala_2+H]^+$. The IR pre-excitation increases the UVPD yield by up to a few times (e.g., 4.5 times at 210 nm). Such pre-excitation broadens and redshifts the narrowband UV transitions in cold aromatic peptides, elevating their absorption at UV wavelengths to the red from (close to) the electronic band origins.[28] The stronger absorption increases the number of UV-excited molecules, evenly scaling up the abundance of all photofragments. The UV/VUV fragmentation band of the peptide bond in Fig. 1a is, however, already very broad and smooth, such that it is unlikely that the observed increase of the fragmentation can be caused by an increase of the UV absorption only. Figure 1b compares the UV fragment mass-spectra of dialanine measured with and without an IR pre-excitation. The abundances of the two main fragments do not scale up proportionally upon the pre-excitation. This observation supports our suggestion that an increase in UV absorption alone cannot explain the increase of the fragmentation and points to the higher dissociation rates in IR-UV excited ions.

Statistical dissociation of a dipeptide in the electronic ground state (subsequent to internal conversion) with $\sim 5 \cdot 10^4$ cm^{-1} vibrational energy should be completed on a microsecond timescale,[29-30] which is much shorter than the time-delay of 1.3 ms between the laser excitation and detection of fragments in our experiments. We therefore suggest that the dissociation may happen in an electronic excited singlet state and/or in a triplet state, where the dissociation rates have to compete with the radiative lifetime of the states (typically tens of ns for singlet, but much longer for triplet states). Additional vibrational energy imported to an ion either by a more energetic UV photon or by an IR pre-excitation would near equally assist in overcoming the

barriers between the excited and dissociative states. A comparison of the blue and red traces in Fig. 1a reveals that the dissociation yields are, indeed, almost the same for UV-only and for IR-UV excitations to the same total energy. The lack of vibrational structure in the UV fragmentation spectrum of the dipeptide suggests that the lifetime of the excited S_1 state is much shorter than its radiative time. This would imply a fast transfer of the excitation to another state, which may mediate the dissociation. We may speculate that the mechanism of VUV/UV photofragmentation of dialanine might be similar to the experimentally proven mechanism of photofragmentation of aromatic peptides, which invokes triplet states as a "storage room" for UV excitation.[31] A comprehensive elaboration of this effect would require theoretical and further experimental studies, which is beyond the scope of our report.

Regardless of its mechanism, the detected significant IR-induced increase in UVPD yield enables vibrational spectroscopy of the dipeptide. Figure 2 shows an IR-UV gain spectrum of $[Ala_2+H]^+$, measured with UV OPO wavelength fixed at 210 nm. Four well-resolved peaks are observed in Fig. 2 in the spectral region, where five NH/OH stretch transitions may appear in each conformer of the ion. IR-IR-UV hole-burning spectroscopy assigns all these peaks to the same single conformer (Figure S2 in SI). Theoretical calculations[9, 32-33] predicted four low-energy conformers of $[Ala_2+H]^+$, and room temperature IRMPD spectroscopy in 6 μm spectral region confirmed the presence of two of them[9]. Regarding the calculated low-energy barrier between these two conformers,[33] we may suggest that the cryogenic collisional cooling in our experiments relaxes the higher-energy conformers that are abundant at room temperature to the single most stable structure detected herein.

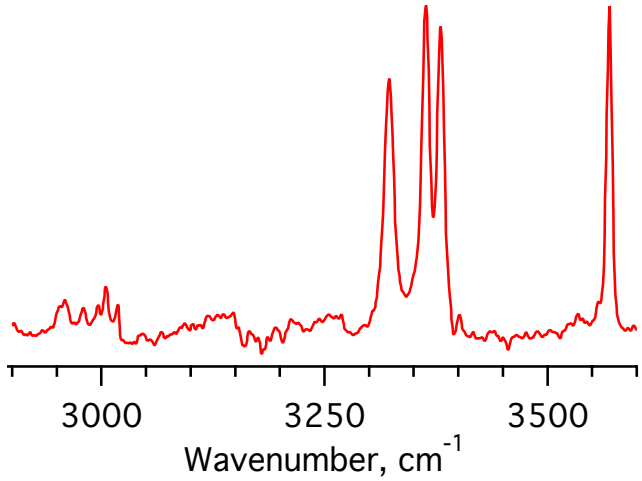

Figure 2. IR-UV gain spectrum of $[Ala_2+H]^+$ recorded by monitoring the intensity of a_1 fragment as a function of IR OPO wavenumber. UV OPO wavelength was fixed at 210 nm.

For a large peptide, an IR-induced relative increase of UV fragmentation yield measured by detecting all photofragments can be substantially lower than with detecting one/few specific fragments. Figure 3 shows an IR-UV gain spectrum of tetrapeptide $[GPGG+H]^+$ recorded by detecting only the most abundant photofragment ($[z_2–H_2O–CO]$), which exhibits a two-fold increase of intensity upon IR pre-excitation (Fig. S3 in SI). A fraction of this spectrum, reproduced in Figure 3 for a comparison, was earlier measured by H_2-tagging technique.[34] The two spectra exhibit the same number and positions of the strongest peaks, although noticeably differ in some details. These differences can arise from different vibrational temperatures of the peptides in the two experiments, reflect the better quality of the IR-UV spectrum, but may also be induced by couplings of the tag to the peptide.

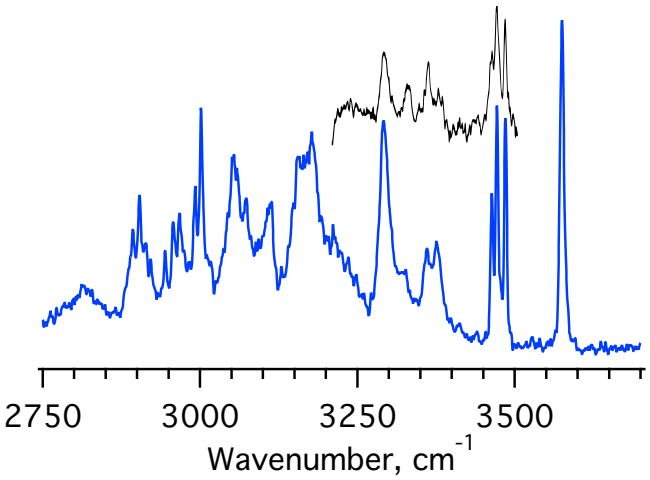

Figure 3. IR-UV vibrational gain spectrum of $[GPGG+H]^+$ (blue trace) recorded by monitoring the intensity of the fragment $[z_2–H_2O–CO]$ (m/z = 70.0 Th) UV OPO wavelength was fixed at 224 nm. The IR spectrum measured by H_2 tagging (black trace) is shown for a comparison (reproduced with permission from ref.[34]).

IR-IR-UV hole-burning spectroscopy may add conformational specificity to the gain spectra, but requires their high quality. The latter may degrade for larger peptides, in particular for cyclic ones, which are difficult to fragment. Many peptide drugs are of cyclic structure, however. This makes spectroscopic studies of this type of molecules particularly important. We have applied conformer-selective vibrational spectroscopy assisted by VUV excitation of peptide bonds to a mid-size non-aromatic peptide cyclo-$[GRGDSP+H]^+$ (m/z = 570.6 Th), which is used in cell biochemistry as a potent vasodilator.[35] UVPD MS of this peptide reveals only one charged fragment (loss of a water molecule by the parent), for which the intensity significantly increases upon IR pre-excitation (Figure S4 in SI). We monitor only this weak fragment for vibrational spectroscopy of the peptide. The black trace in Figure 4 shows the IR-VUV gain spectrum of cyclo-$[GRGDSP+H]^+$ measured with VUV OPO fixed at 194 nm. The highly congested vibrational spectrum suggests the presence of more than one conformer of the peptide.

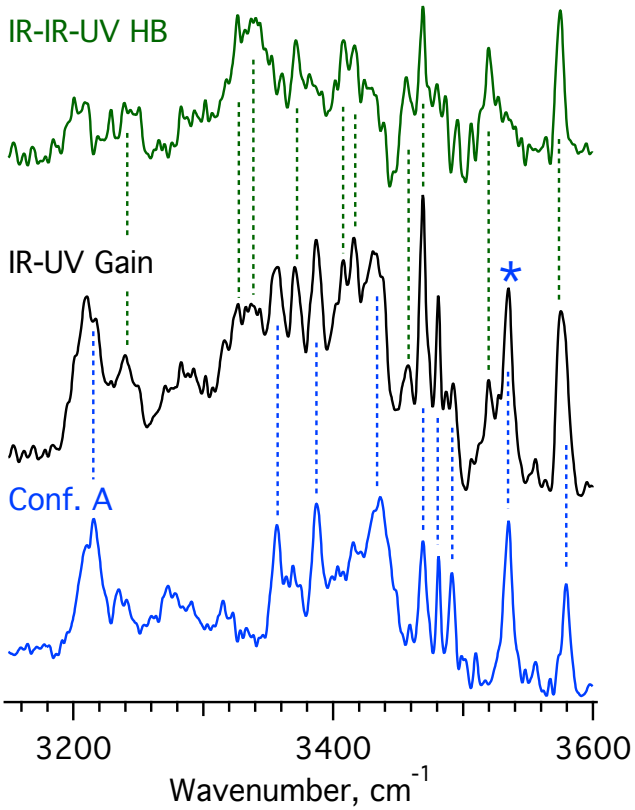

Figure 4. IR-IR-UV hole-burning spectroscopy of cyclo-[GRGDSP+H]$^+$. Black trace – IR-UV gain spectrum; green trace – IR-IR-UV hole-burning spectrum recorded with the pump IR OPO wavenumber fixed at 3535.2 cm^{-1} (transition labelled with an asterisk); blue trace – their difference. UV OPO was fixed at 194 nm.

Partial vibrational resolution in the IR-UV gain spectrum of cyclo-[GRGDSP+H]$^+$ in Figure 4 allows for recording a conformer-selective IR-IR-VUV hole-burning spectrum of this peptide (green trace in Fig. 4) by fixing pump IR OPO wavenumber at one of the resolved transitions. The spectrum of the conformer associated with the labelled transition and named A is obtained as the difference of the IR-UV gain and the IR-IR-UV hole-burning spectra. Cyclo-[GRGDSP+H]$^+$ has ten NH and two OH stretching vibrations, of which as many as nine transitions has been identified for conformer A. The three remaining vibrational transitions might be unresolved or red-shifted due to intramolecular interactions. The IR-IR-UV hole-burning

spectrum contains vibrational signatures of all but one conformers of the ion. At least ten transitions that are not present in the spectrum of conformer A were identified in the hole-burning spectrum (vertical green dashed lines). Similar number of vibrational transitions in the conformer-specific spectrum of the conformer A and in the conformer non-specific spectrum of all other conformers suggests the presence of only two conformers (conformational families). We tentatively attribute the transitions in the IR-IR-UV hole-burning spectrum to the second conformer named B. Regarding the high rigidity of cyclic peptides, it is very likely that conformers A and B (families of conformers) are *trans*- and *cis*- isomers of proline, which are known to be present in Pro-containing peptides.[36]

In conclusion, we have measured a gas-phase VUV/UV photofragmentation spectrum of a single peptide bond in a cryogenically cold protonated dipeptide. The spectrum may serve as a benchmark in proteomics for relating UVPD efficiency at different fixed wavelengths. Despite the cooling, this intrinsic peptide absorption is broad and unstructured. Nevertheless, vibrational pre-excitation of this and larger peptides results in a substantial increase of the yield of some photofragments. This effect enables the demonstrated herein all-conformer IR-UV gain and conformer-selective IR-IR-UV hole-burning vibrational spectroscopy of non-aromatic oligopeptides, The use of peptide bonds as intrinsic UV chromophores makes these techniques a versatile tool of vibrational spectroscopy applicable to, essentially, any small to midsize peptide.

EXPERIMENTAL SECTION

Our tandem mass-spectrometer has been described in details elsewhere.[4] Briefly, ions are transferred from solution to the gas phase using nanoelectrospray ion source. The ions of a specific mass-to-charge ratio are selected with a quadrupole mass filter and guided to the

cryogenic octupole ion trap kept at T=6 K,[26] where they are cooled down to vibrational temperature of ~12 K in collisions with He buffer gas.[2] Once cold, the ions are irradiated with IR and UV OPOs. The parent and fragment ions are released from the trap, the ions of interest are selected in the second quadrupole mass filter, and their intensity is recorded with a channeltron detector as a function of laser wavelength.

IR-UV gain spectrum is recorded with UV OPO (tuned to a fixed wavelength) and IR OPO (scanned over a desired wavenumber range), fired at 10 and 5 Hz repetition rate, respectively. The UV-only and the IR-UV photofragmentation signals are thus recorded in the subsequent experimental cycles.

In IR-IR-UV hole-burning experiments the high-energy (5-10 mJ) pump IR laser is fixed at a vibrational transition that is specific to one of the conformers. The UV OPO and the low-energy (1-2 mJ) scanned IR OPO both fire at 10 Hz, while the pump IR OPO runs at 5 Hz repetition rate. An all-conformer IR-UV gain spectrum and an IR-IR-UV hole-burning spectrum are recorded in the two subsequent cycles. The latter spectrum contains vibrational transition of all conformers, except the one pumped by the pump IR OPO. The difference between the gain and the hole-burning spectra gives a vibrational spectrum of the IR-tagged conformer (see S5 in SI for details).

Sample solutions at the concentration of 50 μM were prepared in HPLC-grade water/methanol/acetic acid (100:100:1 relative volume concentrations) mixture. L-Alanine, dialanine, GPGG, and cyclo-[GRGDSP] were purchased from Carl Roth GmbH & Co. KG, Sigma Aldrich, Bachem Inc., and AnaSpec, respectively, and used without further purification.

ASSOCIATED CONTENT

Supporting Information.

UVPD MS of $[Ala+H]^+$ amino acid, IR-IR-VUV hole-burning spectroscopy of $[Ala_2+H]^+$ and UVPD MS of cold and IR pre-excited peptides $[GPGG+H]^+$ and cyclo-$[GRGDSP+H]^+$, energy diagram for IR-IR-UV hole-burning experiments.

AUTHOR INFORMATION

Notes

The authors declare no competing financial interests.

ACKNOWLEDGMENT

This work was supported by Swiss National Science Foundation (grants 200020_172522 and 206021_164101) and by EPFL.

REFERENCES

(1) Nagornova, N. S.; Rizzo, T. R.; Boyarkin, O. V., Highly Resolved Spectra of Gas-Phase Gramicidin S: A Benchmark for Peptide Structure Calculations. *J. Am. Chem. Soc.* **2010,** *132*, 4040-4041.

(2) Pereverzev, A. Y.; Boyarkin, O. V., Exploring the relevance of gas-phase structures to biology : cold ion spectroscopy of the decapeptide neurokinin A. *Phys. Chem. Chem. Phys.* **2017,** *19*, 3468-3472.

(3) Nagornova, N. S.; Rizzo, T. R.; Boyarkin, O. V., Interplay of Intra- and Intermolecular H-Bonding in a Progressively Solvated Macrocyclic Peptide. *Science* **2012,** *336*, 320-323.

(4) Pereverzev, A. Y.; Cheng, X.; Nagornova, N. S.; Reese, D. L.; Steele, R. P.; Boyarkin, O. V., Vibrational Signatures of Conformer-Specific Intramolecular Interactions in Protonated Tryptophan. *J. Phys. Chem. A* **2016,** *120*, 5598-5608.

(5) Pereverzev, A. Y.; Kopysov, V. N.; Boyarkin, O. V., High Susceptibility of Histidine to Charge Solvation Revealed by Cold Ion Spectroscopy. *Angew. Chem. Int. Ed.* **2017,** *56*, 15639.

(6) Schwing, K.; Gerhards, M., Investigations on isolated peptides by combined IR/UV spectroscopy in a molecular beam – structure, aggregation, solvation and molecular recognition. *Int. Rev. Phys. Chem.* **2016,** *35*, 569-677.

(7) Shubert, V. A.; Zwier, T. S., IR-IR-UV hole-burning: Conformation specific IR spectra in the face of UV spectral overlap. *J. Phys. Chem. A* **2007,** *111*, 13283-13286.

(8) Sohn, W. Y.; Ishiuchi, S.; Carcabal, P.; Oba, H.; Fujii, M., UV-UV hole burning and IR dip spectroscopy of homophenylalanine by laser desorption supersonic jet technique. *Chem. Phys.* **2014,** *445*, 21-30.

(9) Lucas, B.; Grégoire, G.; Lemaire, J.; Maitre, P.; Ortega, J.-M.; Rupenyan, A.; Reimann, B.; Schermann, J. P.; Desfrancois, C., Investigation of the protonation site in the dialanine peptide by infrared multiphoton dissociation spectroscopy. *Phys. Chem. Chem. Phys.* **2004,** *6*, 2659-2663.

(10) Leavitt, C. M.; Wolk, A. B.; Fournier, J. A.; Kamrath, M. Z.; Ganard, E.; Van Stipdonk, M. J.; Johnson, M. A., Isomer-Specific IR-IR Double Resonance Spectroscopy of D2-Tagged Protonated Dipeptides Prepared in a Cryogenic Ion Trap. *J. Phys. Chem. Lett.* **2012,** *3*, 1099-1105.

(11) Johnson, C. J.; Wolk, A. B.; Fournier, J. A.; Sullivan, E. N.; Weddle, G. H.; Johnson, M. A., Communication: He-tagged vibrational spectra of the SarGlyH+ and $H^+(H_2O)_{2,3}$ ions: Quantifying tag effects in cryogenic ion vibrational predissociation (CIVP) spectroscopy. *J. Chem. Phys.* **2014,** *140*, 221101.

(12) Wolk, A. B.; Leavitt, C. M.; Garand, E.; Johnson, M. A., Cryogenic Ion Chemistry and Spectroscopy. *Acc. Chem. Res.* **2014,** *47*, 202-210.

(13) Campbell, E. K.; Holz, M.; Gerlich, D.; Maier, J. P., Laboratory confirmation of C 60 1 as the carrier of two diffuse interstellar bands. *Nature* **2015,** *523*, 322-323.

(14) Voss, J. M.; Fischer, K. C.; Garand, E., Revealing the structure of isolated peptides: IR-IR predissociation spectroscopy of protonated triglycine isomers. *J. Mol. Spectrosc.* **2018,** *347*, 28-34.

(15) Peterson, D. L.; Simpson, W. T., Polarized Electronic Absorption Spectrum of Amides with Assignments of Transitions. *J. Am. Chem. Soc.* **1957,** *79*, 2375-2382.

(16) Clark, L. B., Polarization Assignments in the Vacuum UV Spectra of the Primary Amide, Carboxal, and Peptide Groups. *J. Am. Chem. Soc.* **1995,** *117*, 7974-7986.

(17) Woody, R. W.; Koslowski, A., Recent developments in the electronic spectroscopy of amides and alpha-helical polypeptides. *Biophys. Chem.* **2002,** *101-102*, 535-551.

(18) Ward, J. C., Measurements on ultra-violet dichroism. *Proc. R. Soc. London, Ser. A* **1955,** *228*, 205-219.

(19) Bowers, W. D.; Delbert, S.-S.; Hunter, R. L.; McIver, R. T. J., Fragmentation of Oligopeptide Ions Using Ultraviolet Laser Radiation and Fourier Transform Mass Spectrometry. *J. Am. Chem. Soc.* **1984,** *106*, 7288-7289.

(20) Hunt, D. F.; Shabanowitz, J.; Yates, J. R. I., Peptide Sequence Analysis by Laser Photodissociation Fourier Transform Mass Spectrometry. *J. Chem. Soc., Chem. Commun.* **1987,** *1*, 548-550.

(21) Reilly, J. P., Ultraviolet photofragmentation of biomolecular ions. *Mass Spectrom. Rev.* **2009,** *28*, 425-447.

(22) Choi, K. M.; Yoon, S. H.; Sun, M.; Oh, J. Y.; Moon, J. H.; Kim, M. S., Characteristics of Photodissociation at 193 nm of Singly Protonated Peptides Generated by Matrix-Assisted Laser Desorption Ionization (MALDI). *J. Am. Soc. Mass. Spectrom.* **2006,** *17*, 1643-1653.

(23) Aponte, J. R.; Vasicek, L.; Swaminathan, J.; Xu, H.; Koag, M. C.; Lee, S.; Brodbelt, J. S., Streamlining Bottom-Up Protein Identification Based on Selective Ultraviolet Photodissociation (UVPD) of Chromophore-Tagged Histidine- and Tyrosine-Containing Peptides. *Anal. Chem.* **2014,** *86*, 6237-6244

(24) Fung, Y. M. E.; Kjeldsen, F.; Silivra, O. A.; Chan, T. W. D.; Zubarev, R. A., Facile Disulfide Bond Cleavage in Gaseous Peptide and Protein Cations by Ultraviolet Photodissociation at 157 nm. *Angew. Chem. Int. Ed.* **2005,** *44*, 6399-6403.

(25) Brodbelt, J. S., Photodissociation mass spectrometry: new tools for characterization of biological molecules. *Chem. Soc. Rev.* **2014,** *43*, 2757-2783.

(26) Boyarkin, O. V.; Kopysov, V., Cryogenically cooled octupole ion trap for spectroscopy of biomolecular ions. *Rev. Sci. Instrum.* **2014,** *85*, 033105.

(27) Wetlaufer, D. B., Ultraviolet spectra of proteins and amino acids. *Adv. Protein Chem.* **1962,** *17*, 303-390.

(28) Nagornova, N. S.; Rizzo, T. R.; Boyarkin, O. V., Exploring the Mechanism of IR-UV Double-Resonance for Quantitative Spectroscopy of Protonated Polypeptides and Proteins. *Angew. Chem. Int. Ed.* **2013,** *52*, 6002-6005.

(29) Griffin, L. L.; Mcadoo, D. J., The Effect of Ion Size on Rate of Dissociation - Rrkm Calculations on Model Large Polypeptide Ions. *J. Am. Soc. Mass. Spectrom.* **1993,** *4*, 11-15.

(30) Sun, M. L.; Moon, J. H.; Kim, M. S., Improved Whitten-Rabinovitch approximation for the Rice-Ramsperger-Kassel-Marcus calculation of unimolecular reaction rate constants for proteins. *J. Phys. Chem. B* **2007,** *111*, 2747-2751.

(31) Zabuga, A. V.; Kamrath, M. Z.; Boyarkin, O. V.; Rizzo, T. R., Fragmentation mechanism of UV-excited peptides in the gas phase. *J. Chem. Phys.* **2014,** *141*, 154309.

(32) Marinica, D. C.; Grégoire, G.; Desfrancois, C.; Schermann, J. P.; Borgis, D.; Gaigeot, M. P., Ab Initio Molecular Dynamics of Protonated Dialanine and Comparison to Infrared Multiphoton Dissociation Experiments. *J. Phys. Chem. A* **2006,** *110*, 8802-8810.

(33) Sohn, W. Y.; Lee, J. S., Structure and Conformaional Stability of Protonated Dialanine. *J. Phys. Chem. A* **2010,** *114*, 7537-7543.

(34) Masson, A.; Williams, E. R.; Rizzo, T. R., Molecular hydrogen messengers can lead to structural infidelity : A cautionary tale of protonated glycine. *J. Chem. Phys.* **2016,** *143*, 104313.

(35) Nadanaka, S.; Sato, C.; Kitajima, K.; Katagiri, K.; Irie, S.; Yamagata, T., Occurrence of Oligosialic Acids on Integrin alpha5 Subunit and Their Involvement in Cell Adhesion to Fibronectin. *J. Biol. Chem.* **2001,** *276*, 33657-33664.

(36) Counterman, A. E.; Clemmer, D. E., Cis−Trans Signatures of Proline-Containing Tryptic Peptides in the Gas Phase. *Anal. Chem.* **2002,** *74*, 1946-1951.

Supplementary Information to:

Peptide Bond Ultraviolet Absorption Enables Vibrational Cold-Ion Spectroscopy of Non-aromatic Peptides.

Aleksandr Y. Pereverzev, Vladimir N. Kopysov, and Oleg V. Boyarkin[*]

Laboratoire de Chimie Physique Moléculaire, École Polytechnique Fédérale de Lausanne, Station-6, 1015 Lausanne, Switzerland

[*] Corresponding Author: oleg.boiarkin@epfl.ch

S1. Photofragmentation Mass-Spectra of $[Ala+H]^+$ and $[Ala_2+H]^+$

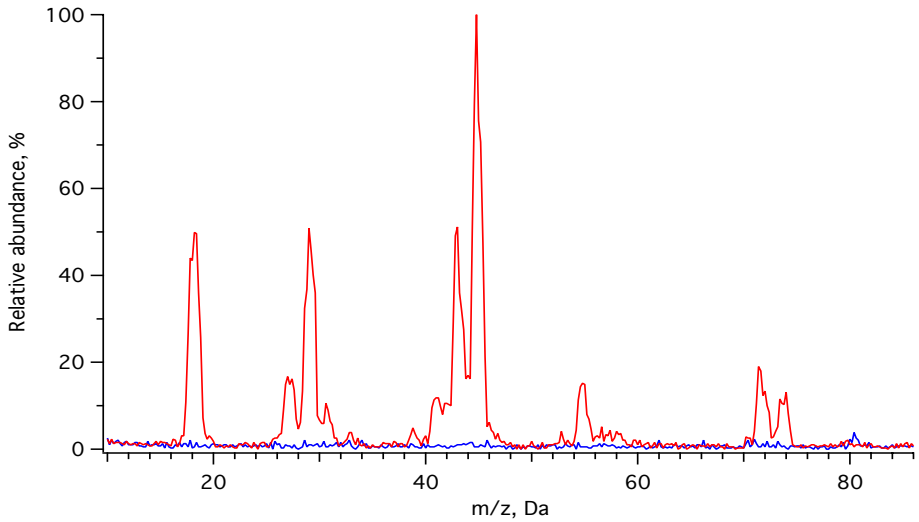

Figure S1. *UVPD (red trace) and CID (blue trace) mass spectra of* $[Ala+H]^+$*. UV OPO wavelength was fixed at 211 nm. Each data point is averaged over 20 measurements and mass increment was 0.2 Da.*

S2. IR-IR-VUV Hole-Burning Spectroscopy of $[Ala_2+H]^+$

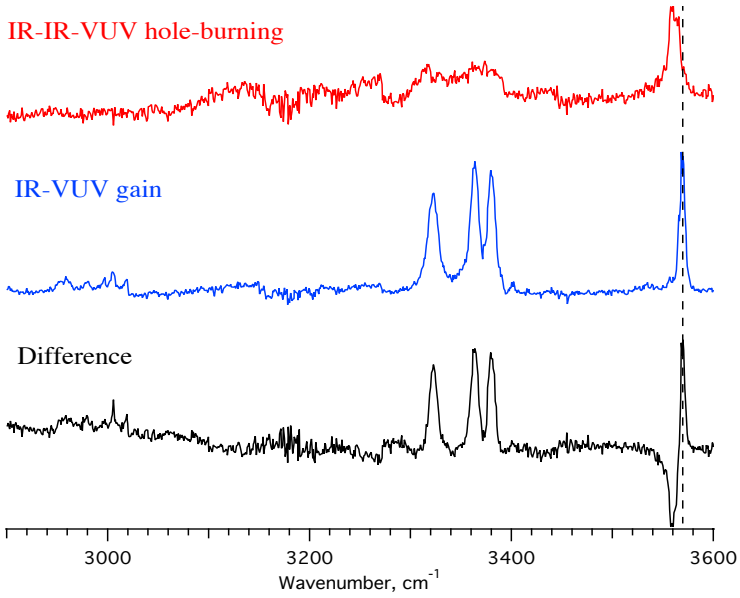

Figure S2. *IR-UV gain (blue trace) and IR-IR-UV hole-burning (red trace) spectra of* $[Ala_2+H]^+$ *recorded with UV OPO wavelength fixed at 210 nm and pump IR OPO wavenumber fixed at 3323* cm^{-1}*. The conformer-specific spectrum (black trace) is generated as the difference of the two curves; the dip at 3560* cm^{-1} *is due 2←1 IR transition and it is shifted from the fundamental transition due to the mode anharmonicity.*

S3. Photofragmentation Mass-Spectrum of $[GPGG+H]^+$

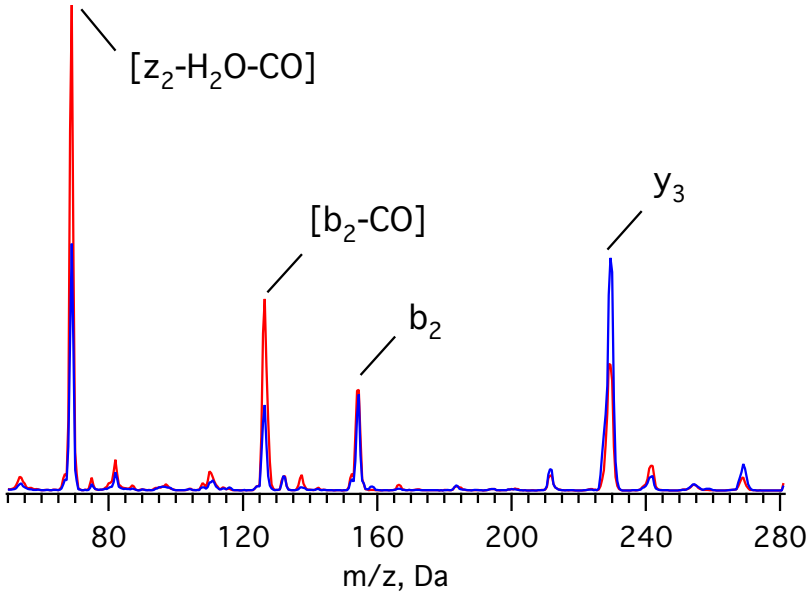

Figure S3. *UVPD mass spectra of cold (blue trace) and IR-preheated (red trace)* $[GPGG+H]^+$*. UV OPO wavelength was fixed at 240 nm and IR OPO wavenumber was fixed at 3575.4* cm^{-1}*. Each data point was averaged over 20 measurements; mass increment was 0.5 Da.*

S4. Photofragmentation Mass-Spectrum of cyclo-$[GRGDSP+H]^+$

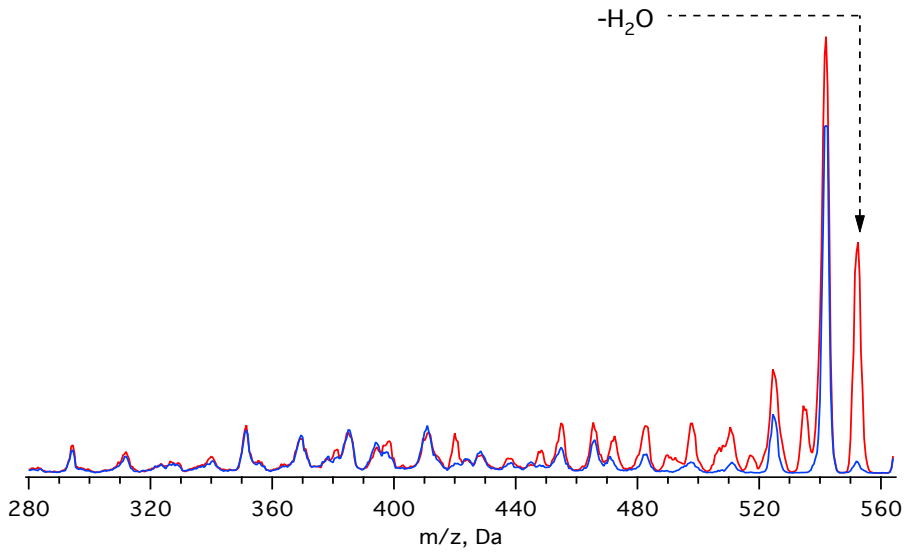

Figure S4. *Photofragmentation mass spectra of cold (blue trace) and IR-preheated (red trace) cyclo-*$[GRGDSP+H]^+$*. UV OPO wavelength was fixed at 196 nm and IR OPO wavenumber fixed at 3573.7* cm^{-1}*. Each data point was averaged over 20 measurements; mass increment was 0.5 Da.*

S5. IR-IR-UV Hole-Burning Spectroscopy

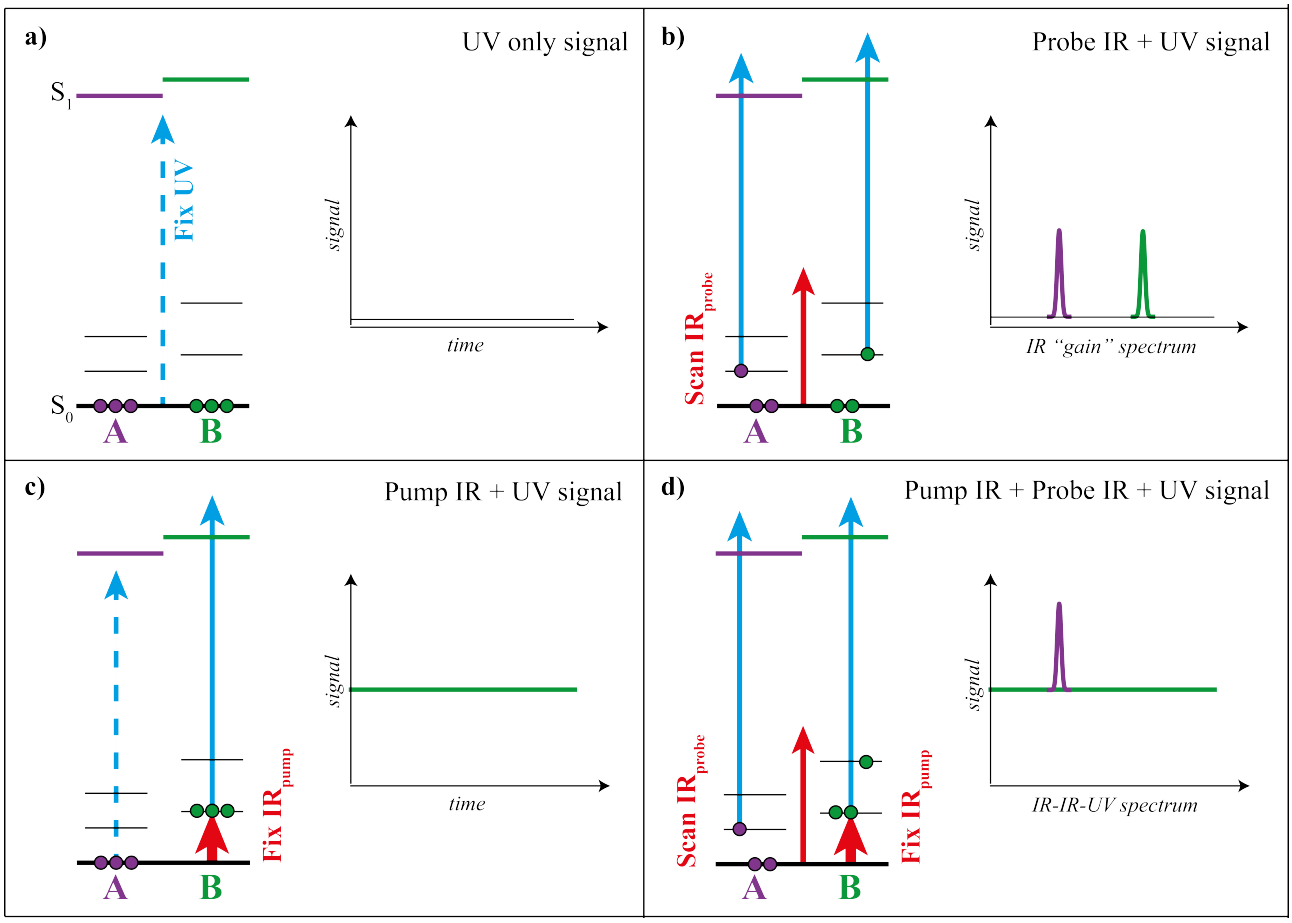

Figure S5. *Schematic explanation of the signal formation principles in the IR-IR-UV hole-burning spectroscopy: (a) UV-only signal; (b) probe IR-UV "gain" signal; (c) pump IR-UV signal; (d) pump + probe IR-IR-UV hole-burning signal.*

Figure S5 explains the principles of the IR-IR-UV Hole-Burning spectroscopy. The UV laser is tuned to the red from a broad UV absorption band, so that the fragmentation signal of the initially prepared ensemble of cold ions with conformations **A** and **B** is negligible (fig. S5a). (NOTE: in the present analysis we assume that the analyte has only two possible structures).

Absorption of the IR photon by any conformer results in an inhomogeneous spectral broadening, which leads to a significant increase of UV-induced photofragmentation. Scanning the wavelength of a probe IR laser, while keeping the UV wavelength fixed, thus, generates an IR "gain" spectrum of all available conformers of an ion at once (fig. S5b).

The pump IR OPO is tuned to a well-resolved vibrational band, specific to one conformer (conformer **B** in fig. S5c). A high-energy pulse of the pump IR OPO laser selectively saturates a

chosen transition creating an ensemble of ions in new state, in which ions of a selected conformer **B** are internally pre-heated, while conformer **A** remains cold. Irradiation of this new ensemble with the UV laser pulse generates a constant non-zero fragmentation signal, which stems only from the conformer **B** tagged by the pump IR laser.

Figure S5d shows the IR-IR-UV hole-burning spectrum, which is essentially a "gain" spectrum of the selectively pre-heated ensemble. If the energy of the pump IR OPO pulse is enough to saturate the corresponding transition of the IR laser-tagged conformer **B,** its UV-induced photodissociation yield of the pump IR pre-heated ions does not change after absorption of the second photon from the probe IR OPO laser pulse. Therefore, all vibrational transitions associated with the conformer **B** disappear in the IR-IR-UV hole-burning spectrum. Since the absorption of conformer **A** does not change after the pump IR OPO pulse was fired, its IR "gain" signal ads to the constant baseline from the conformer **B**. Thus, scanning the probe laser across the whole IR region, while simultaneously keeping the pump IR and UV lasers fixed, generates the IR-IR-UV gain spectrum that contains only the bands associated with all other conformers, except the selected one, on top of this baseline.

The vibrational spectrum of the targeted conformer, that is associated with the pump IR laser-tagged transition, is generated as the difference of the IR-UV "gain" and IR-IR-UV hole-burning spectra, measured as a function of probe IR OPO wavelength.